Degenerate-signal generation in CuCl under nanosecond-excitation conditions

S. S. Montasser* and H. A. El-Kolaly
Laboratory of Laser Physics and its Application, Department of Physics, Faculty of Science, University of Cairo, Giza, Egypt

B. Hönerlage
Institute de Physique et Chimie des Matériaux de Strasbourg, Groupe d'Optique Nonlinéaire et d'Optoélectronique, 5 rue de l'Université, F67084 Strasbourg, France

(Received 5 June 1991)

The theory that was developed for wave-mixing processes with Gaussian pulses is used here for a real nanosecond pulse for comparison with experiment. Good agreement between the theory and the experimental results for CuCl was obtained for the intensity dependence and excitation spectrum of the signal beam. We found the coherence times for the exciton and biexciton states to be 11 and 0.7 ps, respectively.

In a degenerate-four-wave-mixing experiment, a pulsed laser beam is split into two parts, labeled pump and test beams.[1,2] These beams are then focused under a small angle onto a slab of the material, having a thickness of a few micrometers. The nonlinear interaction gives rise to a nonlinear polarization that coherently generates a pulse of the same frequency, namely the signal pulse.[3–8] These three pulses propagate through the sample. In this process, two photons are absorbed from the pump pulse and generation of the signal pulse is induced by the test pulse. A time-resolved investigation of this process was performed by using nanosecond laser pulses close to biexcitonic resonance in CuCl.[9] A theoretical analysis based on the mean-field approximation[10,11] showed that the lifetime of the incoherent quasiparticle population influences the time-dependent generation of the coherent signal. However, the mean-field approximation could not explain the propagation behavior of the fields inside the sample. This was successfully explained by using the slicing model.[12] In this model the sample was considered as if it was cut into slices of variable thickness Δz, the output fields of each slice being the input fields of the next. For each slice the populations and hence the susceptibility χ and the absorption coefficient α are then calculated in terms of the mean field of the incoming pump beam. The slice thickness was chosen such that $\alpha\Delta z \ll 1$. At the front of the sample, the field amplitudes are real but its imaginary parts start growing as the fields propagate through the sample. A Gaussian beam was taken as an input pulse and the temporal and spatial evolution of the field was explained. However, neither the comparison with the experiment nor the study of the excitation spectrum of the signal beams was made. This is the aim of this work.

In our work, instead of the Gaussian beam, we simulate the input pulse shape that is used in the experiment[9] and shown in Fig. 1. Hence we are able to compare it with theory. Otherwise we follow the same procedure as in Ref. 12. We also take into account the effect of reflection from the front side of the sample. This can be done by taking a relatively small time-independent pump intensity and calculate the linear susceptibility. Hence

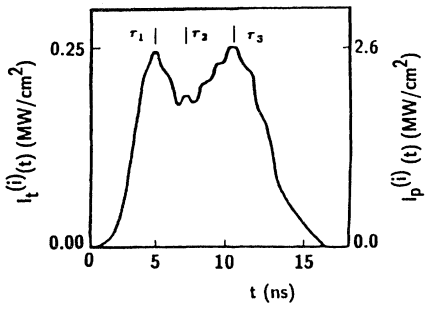

FIG. 1. Temporal shape of the incident pump, $I_p^{(i)}(t)$, and test, $I_t^{(i)}(t)$, pulses.

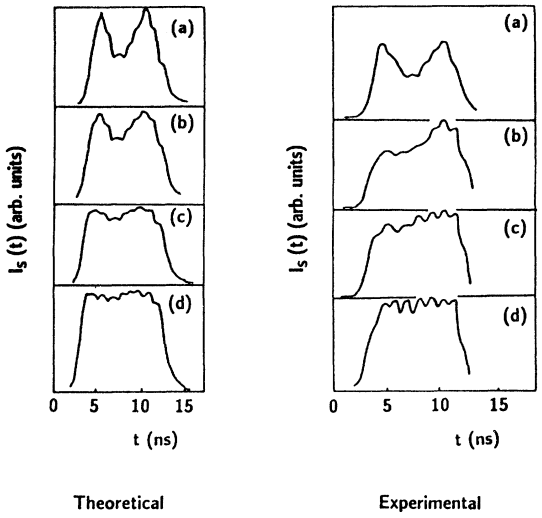

FIG. 2. Shapes of the signal pulse, $I_s(t)$, for different intensities of the pump pulse at a fixed energy $\hbar\omega = 3.185\,66$ eV, where the input pump intensity maximum has the following values in MW/cm^2: (a) 0.24, (b) 1.1, (c) 1.65, and (d) 1.9.

the linear reflection coefficient R can be calculated from the relation

$$R=\frac{(n'-1)+n''}{(n'+1)+n''},$$

where n' and n'' are the real and imaginary parts of the refractive index, which can be calculated in terms of the susceptibility.[13] We will then calculate the excitation spectrum of the signal beam, where we take into account the change of the reflection coefficient.

We take as an input pulse a set of data (200 points) for the pump and test input intensities $I_p(t)$ and $I_t(t)$ extracted from the experimental[9] pulse shape, shown in Fig. 1, by interpolation. These data can then be fed to the first slice as input fields $\{E_p^{(1)}(t)=[(1-R)I_p(t)]^{1/2}\}$ and for the test fields $\{E_t^{(1)}(t)=[(1-R)I_t(t)]^{1/2}\}$. We then follow the slicing model of Ref. 12 in all other respects.

We have calculated the outgoing signal pulse from a 20-μm slab of CuCl at different input maximum intensities and different wavelengths by using the method described above and compared our results with that of Ref. 9. Figure 2 shows the results for the signal beam at different input intensities together with the experimental ones. From this figure we can see that the agreement in the general shape is good. The pulse shape starts from almost the input shape at low intensity to a rectangular shape at high intensity. Figure 3 represents the signal pulse shapes at different wavelengths. In Fig. 3(a) the pulse shape is close to the input one. In Fig. 3(b) the theory could not give the rectangular halves of the experimental one but one may notice the slight separation between the two halves of the theoretical shape. The experimental and theoretical shapes of Fig. 3(c) are almost identical. Very close to resonance [Figs. 3(d)–3(f)] the experimental shapes could not be reproduced by the theory. This gives an indication that another refinement has to be made to the theory. The first half of the pulse shapes in Figs. 3(g) and 3(h) was reproduced by the theory while the second half is higher in the theory than that of the experiment. Finally, in Fig. 3(i) the inputlike pulse shape is reproduced in both theory and experiment.

The time-resolved excitation spectra of the generation rate $G(\hbar\omega,\tau)=I_s(\tau)/I_t^{(i)}(\tau)$ is shown in Fig. 4 in comparison with the experiment at τ_1, τ_2, and τ_3. From this figure we can see that the agreement is reasonable but the relative heights of the two maxima, at energies lower and higher than the resonance points, are reversed.

The spatial evolution of the pump, test, and signal pulse temporal shape inside the sample at $\hbar\omega=3.185\,58$ eV and intensity $I_p=2.6$ MW/cm^2 is shown in Fig. 5. We can see from this figure how the signal pulse shape of the beams evolves from the input pulse shape shown in Fig. 1 to the output rectangular shape shown in Fig. 3(c). It also shows that at the second half of the sample the pump and test beams propagate with almost a constant amplitude.

We have made a comparison between the theoretical model developed by Montasser, Miletic, and Hönerlage[12] and the experimental results of Frindi, Hönerlage, and Levy.[4] Considering the complexity of the processes involved, the agreement is remarkable. In our computation

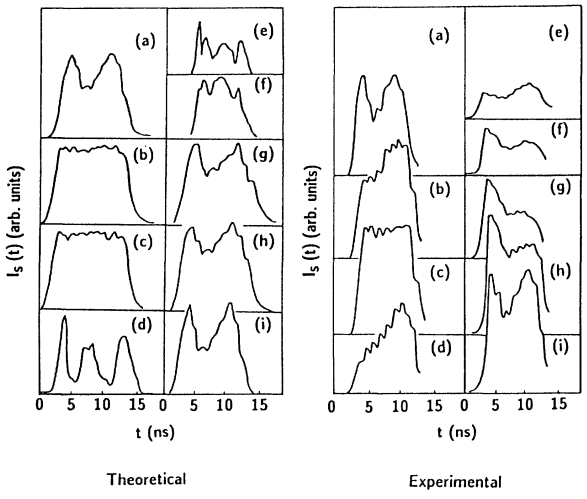

FIG. 3. Shapes of the signal pulse $I_s(t)$, at a fixed input pump intensity maximum of 2.6 MW/cm^2 for the following photon energies in eV: (a) 3.185 25, (b) 3.185 54, (c) 3.185 58, (d) 3.185 77, (e) 3.185 91, (f) 3.186 08, (g) 3.186 24, (h) 3.186 41, and (i) 3.186 74,

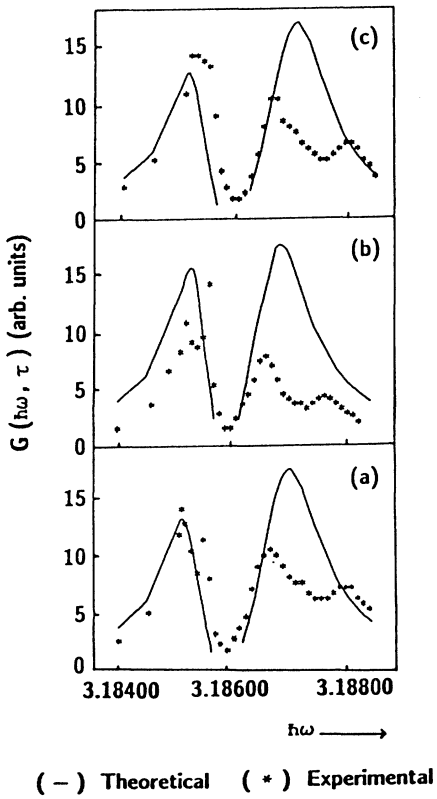

FIG. 4. Time-resolved excitation spectra of the generation rate $G(\hbar\omega,\tau)$ for (a) τ_1, (b) τ_2, and (c) τ_3.

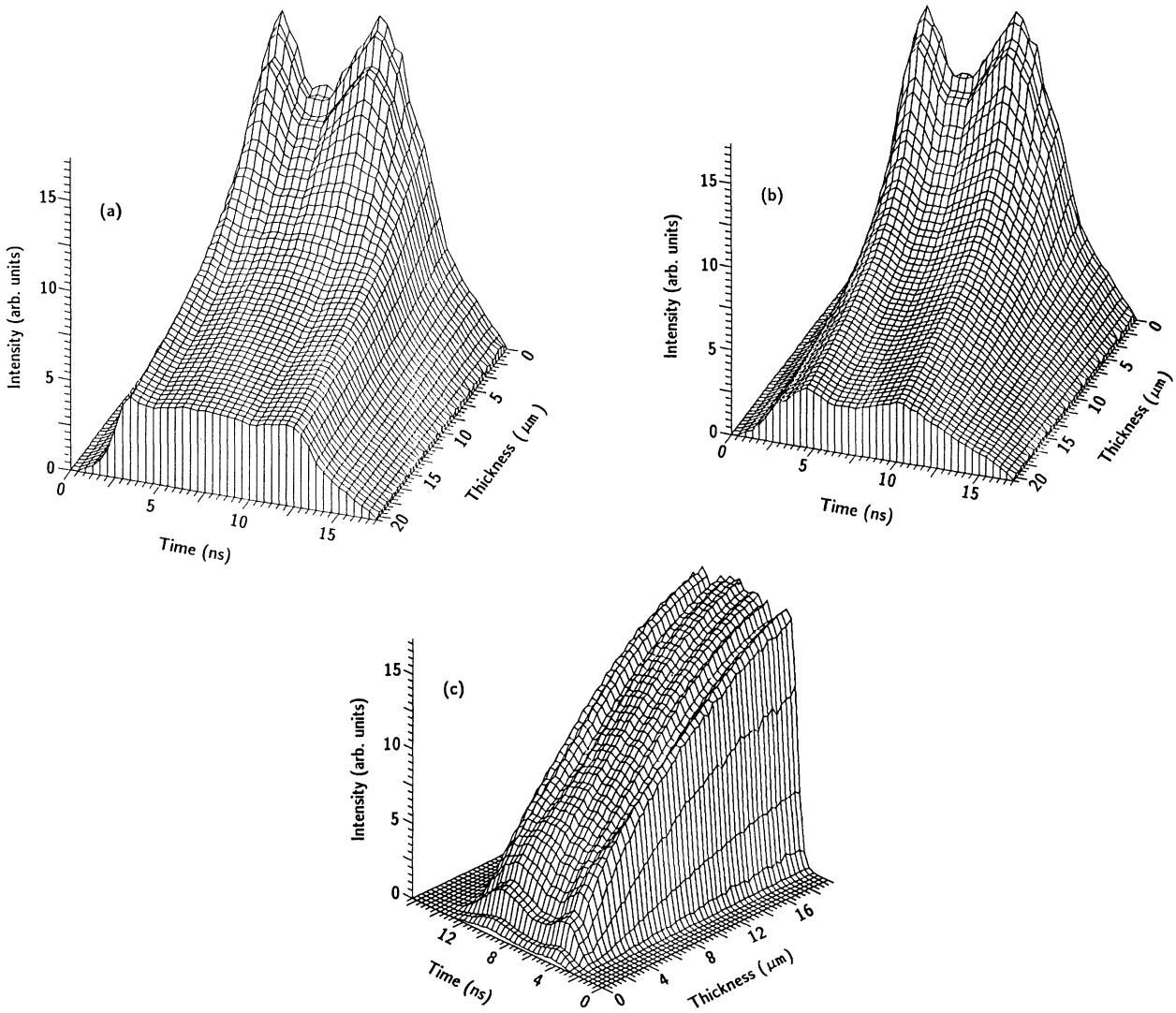

FIG. 5. Spatial evolution of the temporal shape of the (a) pump, (b) test, and (c) signal beams inside the sample at a photon energy of 3.185 58 eV and an input pump intensity maximum of 2.6 MW/cm^2.

we found that the damping parameters, which give good agreement between theory and experiment, yield for the exciton and biexciton coherence times the values $\tau_{ex}=11$ ps and $\tau_{bi}=0.7$ ps. The latter value is quite small when compared to time-resolved, picosecond experiments where coherence times of biexcitons between 10 and 30 ps were found, depending on the excitation intensity.[14,15] We believe that these coherence times evolve during the excitation with the quasiparticle density and the values given here are mean values valid on a nanosecond time scale. The fact that we cannot reproduce the signal shape at resonance is, to our opinion, evidence of the same effect: the damping constants now evolve drastically on a nanosecond time scale during the pulse. Therefore, one should carefully distinguish the time constants determined in nanosecond and picosecond experiment.

The authors would like to acknowledge the help and support of Professor L. El-Nadi and Dr. L. Z. Ismail. This work was supported by The Egyptian Academy of Scientific Research and Technology and the Egyptian National Center of Lasers and its Applications.

*Present address: Department of Physics, Faculty of Science, University of Bahrain, P.O. Box 32038, Bahrain.

[1]A. Marauni, J. L. Oudar, E. Batifol, and D. S. Chemla, Phys. Rev. Lett. **41**, 1372 (1978).

[2]D. S. Chemla, A. Marauni, and E. Batifol, Phys. Rev. Lett. **42**, 1075 (1978).

[3]L. Schultheis, J. Kuhl, A. Honold, and C. W. Tu, Phys. Rev. Lett. **57**, 1797 (1986).

[4]J. M. Hvam, I. Balslev, and B. Hönerlage, Europhys. Lett. **4**, 839 (1987).

[5]T. Yajima and Y. Taira, J. Phys. Soc. Jpn. **47**, 1620 (1979).
[6]G. Grynberg and M. Pinard, Phys. Rev. A **32**, 3772 (1985).
[7]J. W. Haus, C. M. Bowden, and C. C. Sung, Phys. Rev. A **31**, 1936 (1985).
[8]Vu Duy Phach, A. Bivas, B. Hönerlage, and J. B. Grun, Phys. Status Solidi B **84**, 731 (1977).
[9]M. Frindi, B. Hönerlage, and R. Levy, Phys. Status Solidi B **138**, 267 (1986).
[10]B. Hönerlage and J. Miletic, Europhys. Lett. **7**, 19 (1988).
[11]B. Hönerlage, M. Frindi, and J. Miletic, Phys. Status Solidi B **149**, 775 (1988).
[12]S. S. Montasser, J. Miletic, and B. Hönerlage, Phys. Rev. B **40**, 6163 (1989).
[13]J. Y. Bigot, J. Miletic, and B. Hönerlage, Phys. Rev. B **32**, 6478 (1985).
[14]R. Levy, M. J. M. Gomes, B. Kippelen, and B. Hönerlage, Phys. Status Solidi B **158**, 391 (1990).
[15]M. J. M. Gomes, R. Levy, and B. Hönerlage, J. Lumin. (to be published).